PROCEEDINGS, Twenty-First Workshop on Geothermal Reservoir Engineering
Stanford University, Stanford. California, January 27-29. 1997
SGP-TR-IS5

PREDICTING SHALLOW EARTH STRUCTURE WITHIN THE DIXIE VALLEY GEOTHERMAL FIELD, DIXIE VALLEY, NEVADA, USING A NON-LINEAR VELOCITY OPTIMIZATION SCHEME.

William Honjas, Satish K. Pullammanappillil, W. R. Lettis
William Lettis & Associates
Center for Economic Migration and Tomography
1777 Botelho, Suite *262*
Walnut Creek, CA 94596

Gabriel L. Plank, John N. Louie, Richard Schweichert
University of Nevada, Seismological Laboratory
Center for Economic Migration and Tomography
Department of Geological Sciences University of Nevada, Reno 89557

ABSTRACT

We apply a simulated annealing velocity modeling optimization to **22** km of multi-fold seismic reflection data from the Dixie Valley geothermal field. Our methods take into account strong lateral variations in velocity that are assumed not to exist in conventional, post-stack migration processing methods. Simulated annealing is an iterative, computer intensive optimization method for two-dimensional velocity estimation which makes no assumptions on the direction of the sub-surface velocity gradient. Employing this, we can develop velocity models from raw seismic data that accurately represent heterogeneous subsurface structure within thermal anomalies using no a priori data. We correlate velocity structure derived from the Dixie Valley seismic data with known geologic structure and seismic velocities derived from borehole data. Our results indicate six percent or less difference in velocity between models derived from simulated annealing and those derived from examination of well and surface . geological data. Our model also reflects lateral variations in velocity westward toward the surface trace of the Stillwater Fault. We present examples of applying simulated annealing to seismic reflection data from Dixie Valley and from the laterally complex offshore Santa Maria Basin. California.

INTRODUCTION

Recently developed seismic processing methods may allow the reflection seismogram to be used as an effective and economic tool for the exploration and development of geothermal resources. The advent and success of reflection surveying in the petroleum industry illustrates the path of development which could be repeated in the geothermal industry. Formerly, oil exploration concentrated in areas where the resource was somehow manifested at the surface, much as geothermal exploration concentrates on fumaroles and hot springs today. New methods of data processing, such as 3-d imaging and reflection coherency, are everyday increasing the importance of the seismic reflection method by allowing the petroleum industry to expand into ever more complex exploration environments (Thomas, 1996).

Geothermal exploration has generally employed conventional, post-stack seismic reflection processing techniques to attempt to image permeable structures such as faults (Okaya and Thompson, 1985). These conventional reflection processing methods were developed to image earth structure in clastic delta environments, which do not generally possess the inherent lateral velocity variations imposed in more structurally complex geothermal environments.

Conventional seismic reflection processing methods discount the existence of steeply dipping faults and fractures (often permeable features in geothermal settings), and laterally complex geologic structure. Because conventional migration methods use simplistic, sometimes constant layered velocity models to produce images, structures which cause strong lateral variations in velocity are rendered invisible. In this study, initial results of new seismic processing methods are presented. This technology will hopefully increase drill success rates. Examples of the ability of new seismic processing methods to constrain subsurface velocity structure in laterally heterogeneous geologic environments, with no a priori information except the raw shot gathers, are shown (Honjas, 1993; Pullammanappallil and Louie, 1994; Louie et al., 1997).

For this pre-print, the simulated annealing velocity model from Dixie Valley will extend to 1 km depth (Figure 4). The maximum source-receiver offset along Line 10 is about 2.6 km. Hence, by using only first-arrival travel times and reflection coherency of shallow reflectors, we are able to constrain velocities down to 1 km. To date, attempts at using seismic reflection as a tool for geothermal exploration have used processing methods designed by the petroleum industry for application within sedimentary basins. As such, seismic surveys commissioned for geothermal projects focused primarily on collecting reflectivity data. These data generally lack sufficient information to constrain laterally varying velocities at reservoir depths. For geothermal exploration seismic surveys, offsets should be increased to allow velocity sampling of first-arrivals at reservoir depths (2 to **3** km). Additional. constraints can be obtained by including reflection picks. For Line 10, velocity at reservoir depth will be constrained by: Combining first-arrival time and reflection coherency (Pullammanappallil and Louie, 1996); integrating reflection-picks into the velocity inversion which may extend the simulated annealing velocity model to reservoir depth, and by integrating velocities obtained from bore-hole data beneath 1 km depth.

GEOLOGIC SETTING OF DIXIE VALLEY

Dixie Valley is an active Basin and Range graben in west-central Nevada (Figure 1). Roughly 120 km long and 19 km wide, it is bounded to the west by the Stillwater Range and to the east by the Clan Alpine Mountains. The valley supports an elongated geothermal area and maintains a heat flow which is high in relation to the surrounding Battle Mountain heat flow high. The adjacent ranges, which have been uplifted along range-bounding normal faults, reveal a complicated geological history of Phanerozoic thrust faulting, volcanism, and extensional faulting. **In the** northern part of the valley, fumaroles and hot springs occur along the Stillwater range front-fault. Commercial development of the geothermal field began in 1978 with deep exploratory drilling, and today the field supports one 62 Mw plant which became operational in 1988. Lithologic logs from geothermal wells within the present field display spatial inconsistencies in depths to and thicknesses of known rock units (Plank, 1996).

The complex geology exposed in the Stillwater and Clan Alpine ranges are represented within the down-dropped Dixie Valley block, which are buried beneath 1800 meters of Tertiary and Quaternary basin fill deposits. At least two, and possibly four separate tectonic events have affected these rocks. These events span the range from brittle to ductile deformation, and have involved intrusive and extrusive igneous, sedimentary, and metamorphic rocks (Plank, 1997).

Dixie Valley occupies a part of the Central Nevada Seismic Belt: a generally north-northeast trending zone of Quaternary faulting and historical seismicity that has been the locus of several moderate to large magnitude earthquakes during the past 100 years. The

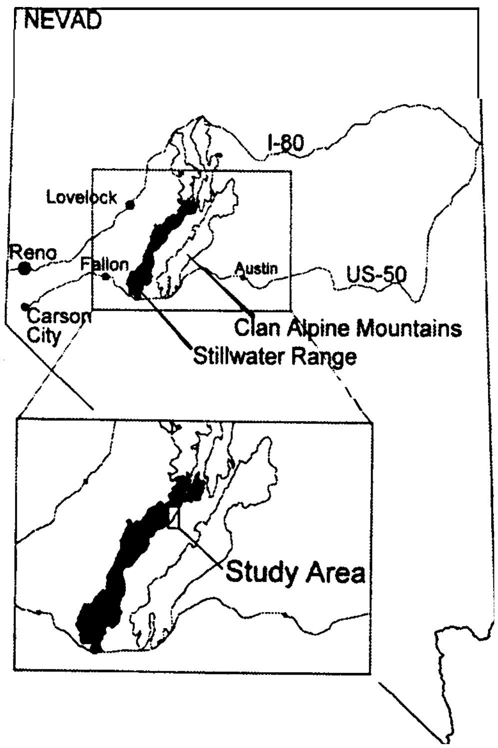

Fig. 1 Location Map

geothermal field is located between the endpoints of the 1954 and 1915 surface ruptures in the Stillwater seismic gap, a segment of the Stillwater Fault which has not ruptured in historic times (Wallace and Whitney, 1984). **It** also may be influenced by several regional structural features (Fonseca, 1988).

DATA AND METHODS

Seismic reflection data from Line 10 Dixie Valley, Nevada, are presented (Table 1) (Figure **2).**

The method we employ creates P-wave, high resolution velocity models using a nonlinear optimization technique based on **a** simulated annealing algorithm. (Pullammanappallil and Louie, 1995). First arrival picks made on raw, unstacked shot gathers are input to the optimization codes. Resulting models show variations in the seismic velocities of reservoir rocks, and constrain the location of tectonic features and other subsurface geologic structure.

The simulated annealing technique is a Monte-Carlo based estimation process that can generate velocity models independent of the initial or starting model, with little or no a priori information (Pullammanappallil and Louie, 1993). An arbitrary starting model is perturbed randomly until the synthetic travel times computed through it match the travel times picked from the data. New models producing less travel time error are accepted for further enhancements, and models having increased error can be accepted conditionally based on their total error. **As** annealing proceeds, conditional acceptance becomes less and less likely. Unlike linearized iterative inversions, simulated annealing optimization will find the global velocity solution while avoiding the local error minima. **It** is also completely insensitive to the starting velocity model. However, the process is very sensitive to the density of data points. Models with little data coverage will develop a large set of different models that will fit the data.

Line Number	Line Length	Source Type	Record Length	Sample Rate	Pattern (CMP)**	Number of Groups	Group Interval	Shot Point Interval	Max. Fold
10	**5.6**	Vibroseis	**16** sec.	**2** msec.	inline	**96**	**165'**	**660'**	**12**

Table 1: Data parameters for Line 10, Dixie Valley, Nevada (Courtesy of Oxbow Geothermal Corp.).

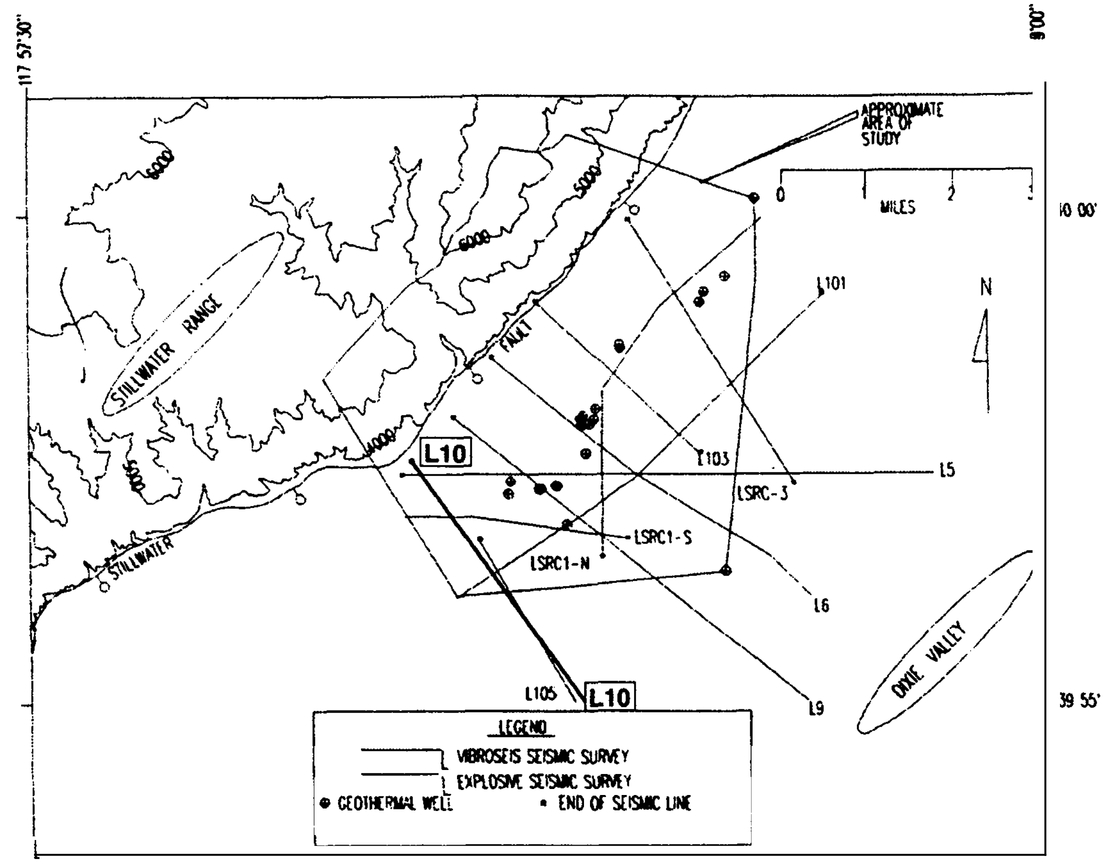

Fig.2. Location Map of Seismic Reflection Lines.

The simulated annealing optimization method simultaneously maximizes reflection coherency while minimizing first-arrival travel time residuals (Pullammanappallil and Louie, 1996). Relatively shallow velocity structure is constrained by first arrival times, while coherency information from deeper reflections (if present) helps constrain deeper velocities. **A** tomogram produced by the optimization process is input into a Kirchhoff pre-stack migration algorithm to image the seismic reflectors directly. This is demonstrated in pre-stack images from the offshore Santa Maria Basin, California (Figure **3).** The velocity model allows accurate calculation of travel times down to and up from every point in the reflection data volume (Louie et al., 1988; Honjas, 1993). Provided an accurate velocity model, pre-stack migration will produce a depth image from the data volume. Conventional, post-stack seismic sections are viewable only as travel time sections. Depth images are directly comparable to other **2-d** images, such as gravity models or geologic cross sections. The pre-stack migration shown in Figure 3(c) reveals a steeply dipping Hosgri fault zone displaying multiple branches (Figure 3(c)). The migrated images agree with corroborating, multi-disciplinary studies of the offshore Santa Maria Basin suggesting that the fault zone displays upward diverging flower structures characteristic of strike-slip faulting (PG&E, 1990).

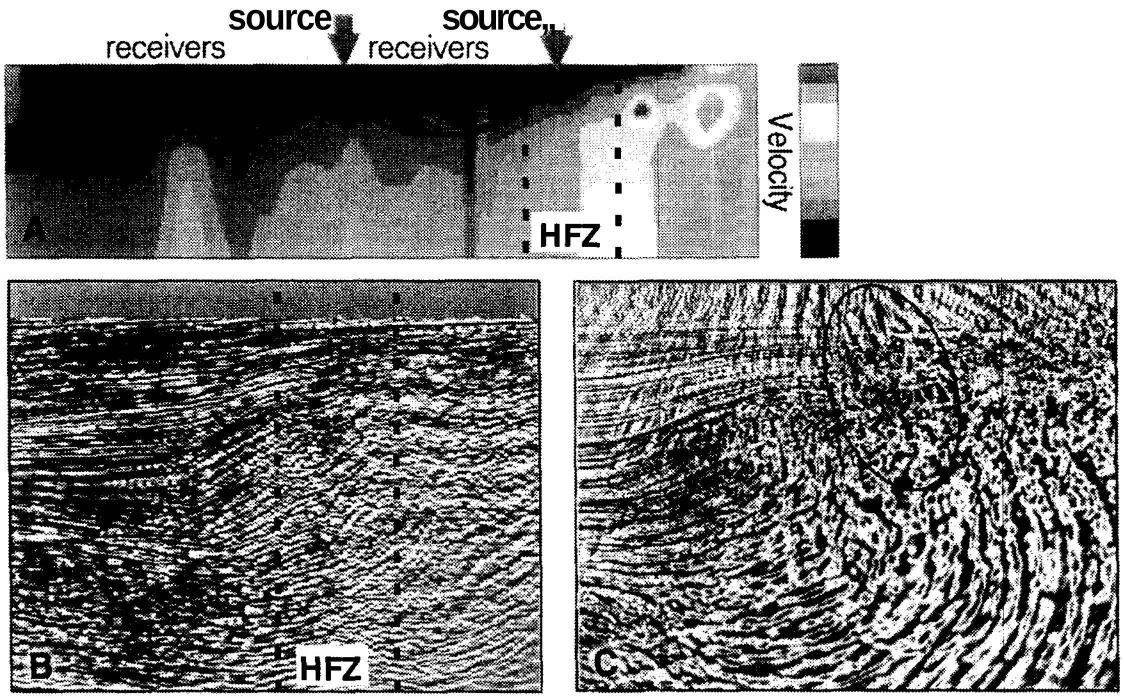

Fig. 3. (a) Simulated annealing velocity model across the Hosgri Fault Zone, offshore Santa Maria Basin, CA. The Hosgri Fault Zone (HFZ) is indicated. Note lateral velocity discontinuity within the HFZ. The velocity model was derived with no a priori geologic data.

(b) Conventional, post-stack image across the Hosgri Fault Zone. The presence of a fault is indicated by bedding truncations and diffraction column. The geometry or presence of multiple fault traces are not revealed.

(c) Pre-stack migration using the velocity model shown in 3(a). The image revealed steeply dipping fault with upward-diverging flower structures, consistent with geologic models across the HFZ.

RESULTS

The velocity models derived from simulated annealing and borehole data for Line 10 are shown in Figures 4(a) and 4(b), respectively. The length of each velocity profile is 4 km. For the purpose of this pre-print, Results of processing data from Line 10 to 1 km depth are shown. First arrival data constrains velocity structure well within the upper 1 km. However, it should be noted that the area within 200 m from each end of the velocity model are poorly constrained due to lack of sufficient ray coverage. The simulated annealing model was created using only first arrival data plus coherency, with no input of a priori data. Also, it is important to note that the velocity cross section is a depth section, and therefore correlations can be made between the velocity structure and lithology.

The geology based velocity model was created using a combination of velocities measured directly from seismic data (from 0.0 to 0.8 km) and velocities derived from bore hole sonic logs (from 0.8 to 1.0 km). The geology based velocity model is a generalized velocity cross section for the valley; the depth boundary for each velocity layer represents averaged velocity values calculated for each depth range, and then projected horizontally. The comparison between velocities from the

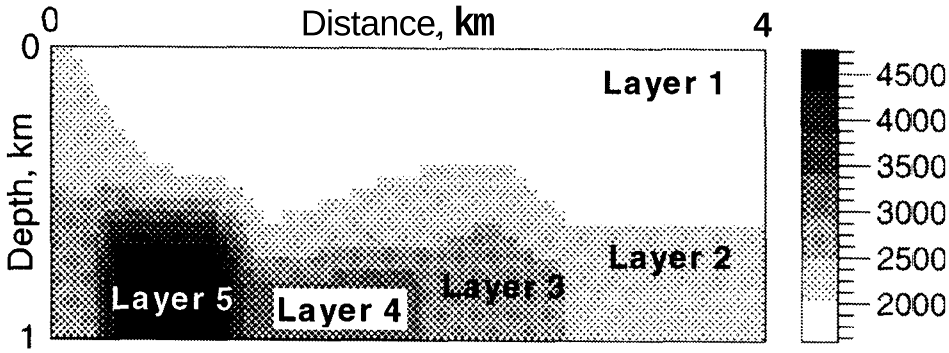

Fig. 4(a). Simulated Annealing Velocity Model; Line 10 Dixie Valley, Nevada.

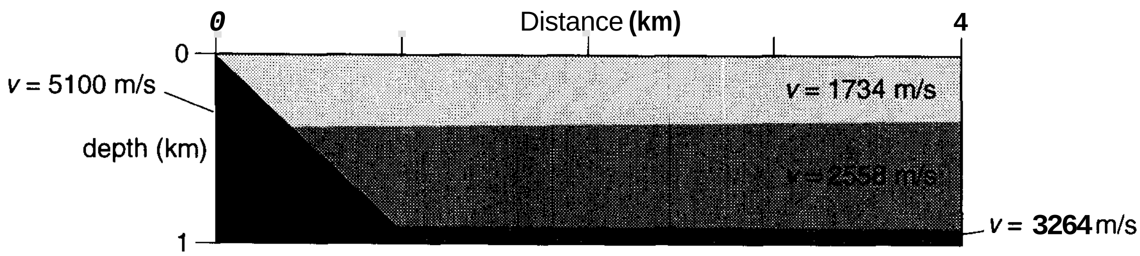

Fig. 4(b). Geology-based velocity model from bore-hole data.

geology-based model and the simulated annealing velocity model are summarized in Table 2.

Four layers dominate the optimized velocity model shown in Figure 4(a), varying from 1.6 to about 3.2 km/s. These velocities are consistent with those for Quaternary basin sediments in Nevada (Louie, 1997). In general, the layers increase in velocity with depth. However, stronger yet are the apparent lateral variations in velocity. Velocities are observed to increase westward toward the surface trace of the Stillwater Fault. Layer 5 has a velocity greater than 4.5 km/s (Figure 4(a)). This high velocity is consistent with Jurassic rocks that have been mapped within the footwall of the Stillwater Fault (Plank, 1997).

DISCUSSION

Table 2 reveals less than a 6 percent difference in velocity structure between the models derived from simulated annealing and from borehole data (Figures 4(a and b)). Velocities from the simulated annealing model correlate well with theoretical velocities calculated for the rock types observed from borehole data (Louie, 1997) (Table 2). The correlations suggest that the velocity structure derived from simulated annealing is reliable.

One striking feature on the simulated annealing velocity model is the abrupt lateral velocity change from about 1.3 to 1.5 km E-W. This change coincides with a slight increase in the depth to velocity layer 2 before it begins to shallow westward toward the surface trace of the Stillwater Fault, which lies about 180 meters off the west end of the cross-section. Similar lateral velocity structure has been modeled through processing of seismic data from Line 9 (Figure 2) (Figure 4(c)). The projected strike of the velocity contact is roughly parallel to the Stillwater Fault. This perhaps suggests the presence of a tectonic structure within the subsurface about 1.5 km southeast of the surface trace of the Stillwater Fault.

Layer Number	Depth Range From Optimization	Velocity From Optimization	Velocity of Geology Based Model	Depth Based on Geol. Mod.	% Diff vs. Vel. Geology	Lithology Based on Simulated Annealing Velocities
1	0 - 490 m	1700 m/s	1730 m/s	0 - 300 m	2	Basin fill sediments
2	490 - 635 m	2262 m/s	2558 m/s	300 - 850 m	6*	Basin fill sediments
3	635 - 722 m	2490 m/s	2558 m/s	300- 850 m	6*	Basin fill sediments
4	722- 1000 m	3100 m/s	3264 m/s	850- 1000 m	5	Basin fill sediments
5	(NA)	4777 m/s	5100 m/s	(NA) (footwall)	6	Metamorphic

Table 2. Comparison of velocity models and projected lithology. Linearly optimized model was derived using no a priori data. (*) Simulated annealing revealed **5** layers displaying lateral variations in velocity, while simple geologically derived velocity model show **4** horizontal layers. The velocities for layers 1 and 2 were averaged for the sake of comparison. Simulated annealing velocities for layers 2 and **3** are consistent with velocities for basin fill sediments.

CONCLUSIONS

Correlation with available geologic and borehole data demonstrates that the simulated annealing algorithm can constrain subsurface velocity structure with no a priori data.

Velocity structure from the simulated annealing model may be correlated with known local lithology to constrain subsurface geologic structure.

In order to obtain the best images of subsurface structure within complex thermal reservoirs, it will be necessary to design data collection parameters that will provide maximum constraint on velocities at reservoir depths, as well as obtaining reflectivity data.

FUTURE WORK

The velocity cross-sections will be extended, using reflection time-picks to constrain velocity structure to reservoir depth (2 to 3 km). Simulated annealing velocity models will then be employed to create pre-stack depth images.

The velocity models and depth sections will then be correlated with known subsurface structure from the Dixie Valley geothermal field. The 2-d interpretations will then be integrated into a 3-d model of the study area, in an attempt to map the subsurface location of faults and fractures within the Dixie Valley geothermal field. Interpretation of the 2-d and 3-d models will be enhanced by close correlation between interpretations of the seismic images derived from this study, and the wealth of corroborating geologic, geophysical, and well data available at Dixie Valley.

ACKNOWLEDGMENTS

This research is funded under the DOE Geothermal Program. We would **also** like to thank Oxbow Geothermal Corp. for allowing us access to all of the data available to Dixie Valley data.

REFERENCES

Fonseca, J. (1988), "The Sou Hills; a barrier to faulting in the central Sierra seismic belt", Journal of Geophysical Research, B, Solid Earth and Planets, 93, 475-489.

Honjas, W. (1993), "Results of post and pre-stack migrations imaging of the Hosgri Fault, offshore Santa Maria Basin, CA" [Masters Thesis]: University of Nevada, 109 p.

Louie, J. N., Clayton, R. W., and Le, B. R. J. (1988), three-dimensional imaging of steeply dipping structure near the San Andreas Fault, Parkfield, California, Geophysics, **53,** 176-185.

Louie, J. N. and J. Qin (1991) "Structural imaging of the Garlock fault, Cantil Valley, California", J. Geophys. Res., 14,461-14,479.

Louie, J. N., Pullammanappallil, S. K., and Honjas, W. (1997) "Velocity models for the highly-extended crust of Death Valley, CA.", Geophysical Research Letters, in press.

Louie, J. N. (1997), Personal Communication.

Okaya, D. A. and Thompson, G. A. (1985) "Geometry of Cenozoic extensional faulting: Dixie Valley, Nevada", Tectonics, **4,** 107-125.

Pacific Gas & Electric (PG&E) attachment GSG Q1-A (1990), "Montage of geophysical data and interpretations, Hosgri fault zone, eastern offshore Santa Maria Basin data base, interpretation procedures, and key observations: Diablo Canyon power plant long term seismic program final report, San Francisco, CA.

Plank, Gabriel (1997), Personal communication.

Pullammanappallil, S. K. and J. N. Louie (1993) "Inversion of seismic reflection travel times using a nonlinear optimization scheme", Geophysics, 1607-1620.

Pullammanappallil, **S.** K. and J. N. Louie (1994), "A generalized simulated-annealing optimization for inversion of first-arrival times", Bull. Seismol. Soc. Am., 1,397-1,409.

Pullammanappallil, S. K., Louie, J. N. (1996), "A combined first-arrival travel time and reflection coherency optimization approach to velocity estimation", Geophysical Research Letters, in press.

Thomas, Katherine (1996) "Seismic Demand Continues", American Association of Petroleum Geologists Explorer, **17,** n. 11, 2p.

Wallace, R. E. and Whitney, R. A. (1984), Late Quaternary history of the Stillwater seismic gap, Nevada, Bulletin of the Seismological Society of America, **74, 301-314.**